acta medica

ORIGINAL ARTICLE

Conventional to Early Phase Standardized Uptake Value Ratio on ^{18}F FDG PET/CT Could Reflect Prognosis in Patients with Non-small Cell Lung Cancer

Osman Kupik[1], [MD]
ORCID: 0000-0001-9473-7940

Sertaç Asa[2], [MD]
ORCID: 0000-0003-4060-9331

Gülnihan Eren[3], [MD]
ORCID: 0000-0002-3315-3893

[1]Department of Nuclear Medicine, Faculty of Medicine, Sıtkı Koçman University, 48000, Muğla, Turkey.

[2]Department of Nuclear Medicine, Cerrahpasa Medical Faculty, Istanbul University-Cerrahpasa, 34093, Istanbul, Turkey.

[3]Department of Radiation Oncology, Faculty of Medicine, Sıtkı Koçman University, 48000, Muğla, Turkey.

Corresponding Author: Osman Kupik
Sıtkı Koçman University, Faculty of medicine, Department of Nuclear Medicine, 48000, Muğla, Turkey.
E-mail: osmankupik@gmail.com

https://doi.org/10.32552/2021.ActaMedica.583

Received: 29 December 2020, Accepted: 8 April 2021, Published online: 23 June 2021

ABSTRACT

Objective: A high metabolism/perfusion rate in the tumor is known to be factor indicating poor prognosis. The goal of this study was to investigate the prognostic value of the ratio of the conventional standard uptake value to early-phase imaging standard uptake value in patients with newly diagnosed non-small cell lung cancer.

Materials and Methods: Early-phase imaging was obtained in the first 120 seconds and conventional imaging was taken after median 66 minutes. The ratio of the conventional standard uptake value to early-phase imaging standard uptake value was calculated. Univariate and multivariate analyses were performed using the Cox proportional hazards regression model to assess the relationship between progression-free survival and ratio of the conventional standard uptake value to early-phase imaging standard uptake.

Results: A total of 77 patients with non-small cell lung cancer were recruited. Progression-free survival analysis was performed in 52 inoperable patients. Progression-free survival was found to be related to conventional standard uptake value ($p<0.001$), tumor size ($p<0.001$) and ratio of the conventional standard uptake value to early-phase imaging standard uptake in univariate analysis ($p=0.047$). In the multivariate analysis, ratio of the conventional standard uptake value to early-phase imaging standard uptake ($p=0.001$, HR=1.145, 95CI%:1.145-1.719) and tumor size ($p<0.001$, HR=1.026, 95CI%:1.007-1.045) were found to be independent poor prognostic factors.

Conclusion: The ratio of the conventional standard uptake value to early-phase imaging standard uptake was found an indicator for prognosis. Evaluating the early phase imaging, without a need for kinetic program or software, without disrupting the routine functioning of the clinic, with conventional imaging may contribute to cancer patient management. There is a need for studies with larger groups of patients.

Keywords: Non-small cell lung carcinoma, prognosis, positron emission tomography, perfusion, metabolism.

INTRODUCTION

^{18}F-fluorodeoxyglucose (^{18}F FDG) shows glucose metabolism in the tissue. Tumor glucose metabolism in non-small cell lung cancer (NSCLC) has been shown to significantly affect the biologic behavior of the tumor and a correlation between the maximum standardized uptake value (SUV_{max}) and tumor aggressiveness [1-3]. Decreased blood flow in the tumor leads to hypoxia [4, 5]. Cancer cells develop an adaptation to hypoxia [6]. It is known that low oxygen levels reduce the distribution of chemotherapeutics [7] and that hypoxic tissues are more resistant to radiotherapy (RT) [8]. Some authors recommend to identify hypoxic regions within the tumor and escalate RT doses for these regions [9].

^{18}F-FDG positron emission tomography/computed tomography (^{18}F-FDG PET/CT) early-phase (0-2min) images have been reported to reflect perfusion [10, 11]. The mismatch between early-phase images and conventional images reflects hypoxia [12, 13]. Combined perfusion and metabolism imaging is recommended in clinical studies evaluating the effectiveness of anti-angiogenic therapy [14]. If tumor blood flow could be monitored noninvasively, it might be possible to obtain more information about the effectiveness of the treatment [15].

The purpose of our study was to investigate the prognostic value of the ratio of early phase imaging SUV (SUV_E) values, which can be obtained without need for an expensive kinetic PET program and computer software, to conventional SUV values (SUV_L), for progression free survival (PFS) in patients with newly diagnosed NSCLC.

MATERİALS and METHODS

Ethical approval

The Clinical Research Ethics Committee of our institute reviewed and approved this study (no: 2019/50). Informed consent was obtained from all individual participants included in the study. All procedures performed in studies involving human participants were in accordance with the ethical standards of the institutional and national research committee and with the Helsinki declaration and its later amendments or comparable ethical standards

Patients and Study Design

Patients in whom ^{18}F FDG PET/CT imaging was performed with indications of the characterization of lung mass/nodule and for lung cancer staging between December 2015 and April 2017 were included in the study. Lung cancer diagnosis was histopathologically confirmed in all patients. We evaluated early and conventional ^{18}F FDG PET/CT images of 77 patients with NSCLC. We did not include 12 patients; who had brain metastasis at the time of diagnosis (n: 7), died due to non-disease related reasons (n= 2), and were lost to follow-up (n= 3). We excluded 13 operable patients who had surgical treatment. We included stage II patients who were not candidate for operation due to medical comorbidities and inoperable stage III-IV patients in PFS analysis (n=52).

Patient Follow-up

PFS was calculated from the date of diagnosis to the date of progression of the disease (new lesion or expansion of the previous existing lesion) or to the date of recurrence, or to the date of death associated with the disease. The period from the date of diagnosis to the last follow-up was calculated in patients who survived or in whom progression was not observed. Follow-up of the disease was conducted using conventional CT and/or ^{18}F-FDG PET/CT.

^{18}F-FDG PET/CT Procedures

A PET/CT scanner Biograph mCT (Siemens Healthcare, Erlangen, Germany) was used. After at least 6 hours of fasting, patients with a blood glucose level of <200 mg/dl were administered a FDG injection at an approximate dose of 3.7 MBq/kg. After median 63 minutes [min-max 54-79 minutes] imaging was performed in the supine position with arms up. PET imaging was adjusted to 2 minutes per bed position. Low dose CT parameters: voltage, 120 kV; CARE Dose 4D mA tube current; and slice thickness, 5.00 mm.

Image Analysis

Two nuclear medicine specialists with 9 and 10 years' PET/CT experience (O.K, S.A) and a radiation oncologist with 10 years' experience (G.E) reviewed all ^{18}F-FDG PET/CT images on a

dedicated Workstation (Syngo-via). Early-phase and conventional images were simultaneously evaluated and volumetric areas of the tumor were delineated. Early-phase imaging SUV (2 min. postinjection; SUV_E) and conventional imaging SUV (median 66 min. postinjection; SUV_L) values were calculated. Ratio values (SUV_R) were obtained by dividing conventional imaging SUV values by the early-phase imaging SUV (SUV_L/SUV_E) (Figure 1).

Statistical Analysis

Variables were compared using either Student's t-test or nonparametric tests, depending on the normality of the distribution. Univariate and multivariate analyses were performed using the Cox model to assess the relationship between survival and ^{18}F FDG PET/CT parameters. Any variable with $p<0.2$ in the univariate model was included in the multivariate Cox proportional hazards regression model. For multivariate analyses, the full model included all the variables that we studied, and the final model was constructed using the backward stepwise procedure. Differences between groups were investigated using the log-rank test. Receiver operating characteristic (ROC) curve analysis was used to determine the optimal cutoff value of the SUV_R for PFS. Kaplan–Meier curves were drawn using defined cutoff values and PFS was interpreted using log-rank analysis. Correlation between groups was evaluated using Spearman correlation for non-parametric variables and the Pearson correlation coefficient for parametric variables. All analyses were performed using SPSS v.22 (SPSS, Inc., Chicago, IL), and two tailed $p<0.05$ was considered significant.

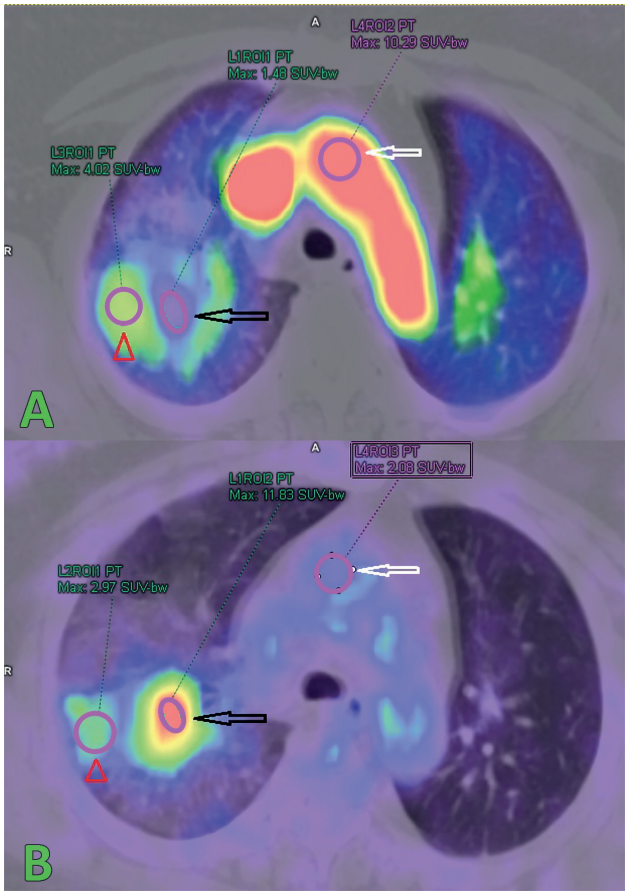

Figure 1. A 66-year-old female with adenocarcinoma. (A) Low FDG uptake (SUV_{max}: 1.48) is observed in the tumor of the early-phase imaging (black arrow). More intense FDG uptake is shown in the atelectasis around the tumor than the tumor itself (SUV_{max}: 4.02) (red arrowhead). Intense blood-pool FDG activity is demonstrated in arcus aorta (SUV_{max}: 10.29). (B) On conventional PET/CT fusion images, a high FDG uptake (SUV_{max}: 11.83) is observed in the tumor (black arrow). The FDG uptake in the atelectasis (SUV_{max}: 2.97) (arrowhead) and aorta (SUV_{max} 2.1) (white arrow) are decreased. Early-phase and conventional imaging look inverslike. Tumor SUV_R =11.83/1.48= 7.99.

RESULTS

Early phase and conventional ^{18}F FDG PET/CT Images of 77 patients with newly diagnosed NSCLC were evaluated [7 women, 70 men, 47 patients (61%) had adenocarcinoma, 30 patients (39%) had SCC, mean age was 65.9±10.23]. The values of the SUV parameters and tumor size are given in Table 1. There was no statistically significant difference in SUV values between groups of patients with adenocarcinoma and SCC ($p>0.05$). In patients with SCC, the tumor size was statistically significantly larger ($p=0.027$).

Relationship between Early-phase Imaging and Conventional Imaging FDG uptake

Among the 77 patients, we found no statistically significant relationship between early-phase imaging and conventional imaging SUV values ($r=0.177$, $p=0.125$). Early phase and conventional SUV values of 77 patients are given in figure 2. When the patients were divided into two groups according to the primary tumor size, the group with a tumor size ≤3 cm comprised 21 patients (27.3%), and the group with a tumor size >3cm constituted 56 patients (72.7%). We found a statistically significant moderate correlation ($r=0.443$, $p=0.044$) between SUV_E and SUV_L values in the group with a tumor size ≤3 cm, whereas there was no correlation in the group with a tumor size >3 cm.

Table 1. The average values of the SUV parameters and tumor size in whole patients, in patient with adenocarcinoma and squamous cell carcinoma (n=77). There was no statisticaly significant difference in SUV values between patients with adenocarcinoma vs squamous cell carcinoma.

Parameter	All Patients (n=77) mean±SD/meadian [min-max]	Adenocarcinoma (n=47)	Squamous cell carcinoma (n=30)	*p**
SUV_E	2.9 (1.3-5.8)	3.051±0.813	2.70 (1.6-5.8)	0.702
SUV_L	14.1 [2.7-42.8]	13.5 (2.7-42.8)	15.05±6.27	0.289
SUV_R	4.94 ± 2.18	4.816±2.187	5.144±2.189	0.522
Tsize (mm)	42 [17-121]	38 (17-121)	50.4±19.55	**0.027**

*p values of adenocarcinoma vs SCC

Abbreviations: SD; standart deviation, SUV_E; early phase imaging standardized uptake value (SUV), SUV_L; conventional imaging SUV, SUV_R; the ratio of SUV_L to SUV_E (SUV_L/SUV_E), Tsize; The longest diameter of the primary tumor.

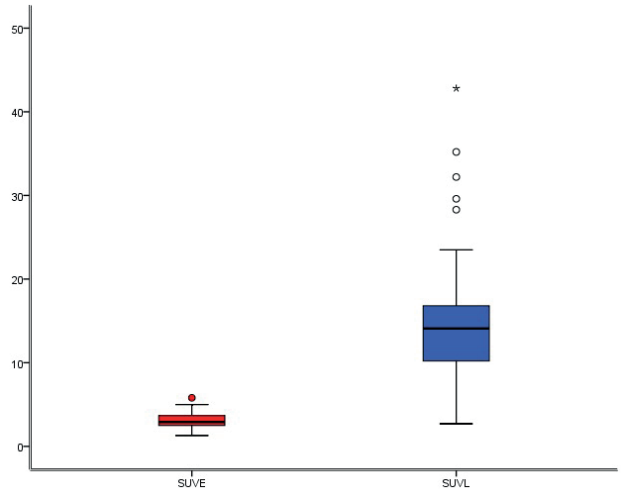

Figure 2. Box-plot graph is showing early and conventional SUV values of 77 patients.

Relationship between Tumor Size and Conventional Imaging/Early-phase Imaging FDG Uptake Ratio

The images of 77 patients were evaluated. Conventional/early-phase imaging FDG uptake ratio increased as tumor size increased. The conventional imaging/early-phase imaging FDG uptake ratio was higher in the group with tumor size >3 cm (p=0.047). Then we divided the patients into 2 groups with tumor size <5 cm and ≥5 cm and found that the conventional imaging phase/ early-phase imaging FDG uptake ratio was higher in the group with tumor size ≥5 cm (p=0.003). Thus, as tumor size increased, the conventional imaging/ early-phase imaging FDG uptake ratio increased (Table 2).

Progression-free Survival Analysis

Fifty-two NSCLC patients who were treated with chemotherapy and /or radiotherapy were included in the study [6 women, 46 men, 28 patients (53.8 %) had adenocarcinoma, 24 patients (46.2%) had SCC, mean age was 66.5±10.25].

Table 2. The relationship of the mean values of SUVR regarding tumor size.

SUVR		
T size	Mean±SD	p
≤ 3cm	3.67±1.85	0.047
>3cm	4.65±1.96	
<5cm	3.92±1.92	0.003
≥5cm	5.28±1.79	

Abbreviations: SUV_E; early phase imaging standardized uptake value (SUV), SUV_L; conventional imaging SUV, SUV_R; the ratio of SUV_L to SUV_E (SUV_L/SUV_E).

Tsize (p< 0.001, HR = 1.038, 95CI%: 1.021-1.056), SUV_L (p< 0.001, HR= 1.155, 95CI%: 1.091-1.224) and SUV_R (p= 0.001, HR= 1.515, 95CI%: 1.251-1.835) were found to be poor prognostic factors for PFS in univariate Cox regression analysis. SUV_E and histological subgroup were not found statistically significant prognostic factors for PFS in univariate Cox regression analysis (p= 0.882, HR= 1.028, 95CI%: 0.716-1.475 and p=0.101, HR=1.781, 95CI%: 0.894-3.547 respectively)

We created a model for multivariate cox regression analysis with Backward LR method. We examined high intercorrelation (multicollinearity) between SUV_L and SUV_R values (correlation matrix of regression coefficient >0.6), thus SUV_L was excluded and only SUV_R was counted in the multivariate cox regression model. In multivariate Cox proportional regression analysis SUV_R (p=0.001, HR=1.145, 95CI%:1.145-1.719) and T size (p=0.007, HR=1.026, 95CI%:1.007-1.045) were found to be independent poor prognostic predictors. Histological subgroup was not independent prognostic factor in the multivariate analysis (p=0.889, HR=0.948, 95CI%:0.446-2.015) (Table 3). Receiver operating

Table 3. The summary of univariate and multivariate Cox regression analysis for progression free survival.

	Univariate Analyse			Multivariate Analyse		
	p	HR	95CI%	*p*	HR	95CI%
SUV_E	0.882	1.028	0.716-1.475	-	-	-
SUV_L	<0.001	1.155	1.091-1.224	*	*	*
SUV_R	<0.001[a]	1.515	1.251-1.835	0.001	1.415	1.145-1.749
Tsize	<0.001[a]	1.038	1.021-1.056	0.007	1.026	1.007-1.045
Histological subgroup	0.101[a]	1.781	0.894-3.547	0.889	0.948	0.446-2.015

*We examined high intercorrelation (multicollinearity) between SUV_L and SUV_R values (correlation matrix of regression coefficient >0.6), thus SUV_L was not included in the multivariate cox regression model.

([a]) indicates parameters included in multivariate analysis.

Abbreviations: 95CI%; 95% Confidence Interval, HR; Hazard ratio SD; standart deviation, SUV_E; early phase imaging standardized uptake value (SUV), SUV_L; conventional imaging SUV, SUV_R; the ratio of SUV_L to SUV_E (SUV_L/SUV_E),Tsize; The longest diameter of the primary tumor.

characteristic (ROC) curve analysis was used to determine the optimal cut-off values of SUV_R for PFS. Patients were divided into two groups as having SUV_R equal to or less than 3.67 or greater than 3.68 (sen-sitivity: 74.3%, specificity: 70.1%, AUC= 0.783, p= 0.001). Kaplan–Meier curves were drawn using defined cutoff values, and 1-year PFS was interpreted using log-rank analysis. The 1-year PFS for the group of patiens with SUV_R ≤3.67 and SUV_R>3.67 were 84.9% and 48.2% respectively (p<0.001) Figure 3.

DISCUSSION

In this study, we investigated the prognostic value of conventional imaging/early phase imaging FDG uptake ratio and the relationship between early phase and conventional imaging SUV values, according to the tumor size, in patients with newly diagnosed NSCLC. This method has never been investigated previously in this group of patients.

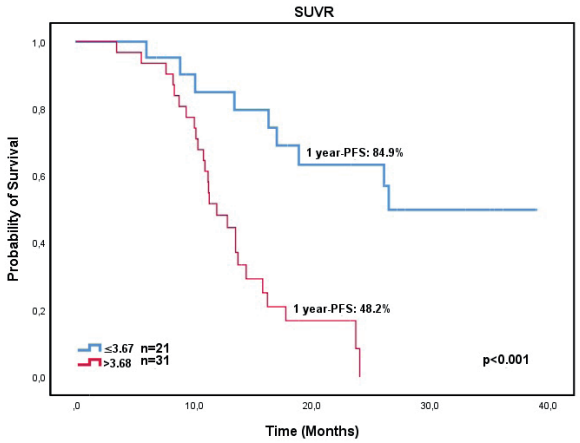

Figure 3. Kaplan-Meier curve for SUVR with the cut-off as 3.67 for progression free survival.

^{18}F-FDG PET/CT early-phase (0-2minutes) images show perfusion, whereas conventional images show metabolism [10, 11]. The mismatch between early-phase imaging and conventional imaging reflects hypoxia [12, 16], which is a predictor for response to radiotherapy and chemotherapy. Low oxygen levels have been shown to decrease the effectiveness of radiotherapy and chemotherapy [7, 17]. A high metabolism-perfusion ratio in head and neck tumors has been shown to be an independent poor prognostic factor for local control [18]. Komar et al. stated that the lack of tumor perfusion in pancreatic cancer caused resistance to chemotherapy, and that this led to a decrease in treatment effectiveness and a poor prognosis [14]. Park et al. showed that high perfusion in pancreatic cancer was associated with an increased CRT response [19]. Aoki et al. investigated the relationship between the average iodine density (AID) obtained from dual energy computerized tomography (DECT), SUV_{max} value, and local control in 74 patients with NSCLC undergoing stereotactic body radiotherapy (SBRT). They found that local control of patients with high SUV and low AID values was worse, and proposed different fractionation schemes for this subgroup [20]. Mankoff et al. showed that patients with breast cancer with high glucose metabolism/perfusion ratio responded worse to treatment [21].

In this study, we obtained ratio values by dividing the conventional imaging FDG uptake value by the early-phase imaging (0-2 minutes) FDG uptake value. In univariate Cox proportional hazard regression analysis, SUV_R, SUV_L and Tsize were associated with PFS, meaning that the prognosis worsened as the conventional imaging/early-phase imaging FDG uptake ratio increased. In this aspect, our result was consistent with studies

stating that the metabolism-perfusion mismatch was associated with poor prognosis.

Tissue perfusion and vascular permeability can be measured using dynamic contrast-enhanced MRI, ^{15}O-water PET, perfusion CT, and dynamic ^{18}F-FDG PET. It is assumed that ^{18}F FDG is transported from the blood into the tissue at a linear transfer rate K1 relative to the blood flow. K1 which is a measure of capillary permeability and perfusion has been shown to have prognostic value in the treatment of cancer [22]. In a study with patients with soft tissue sarcoma, Okazumi et al. suggested that SUV and K1 should be evaluated together for more accurate results [23]. Strauss et al. showed that there was a correlation between FDG K1, vascular endothelial growth factor (VEGF), and angiopoietin in patients with colorectal cancer, concluding that angiogenesis was a determining factor for FDG PET kinetics [24]. There is a strong correlation between the K1 value obtained from dynamic FDG PET early-phase imaging (0-2 minutes) and the flow measured with ^{15}O water PET. Thus, tumoral perfusion would be evaluated with the FDG PET obtained in the first-pass FDG uptake (K1). A single ^{18}F-FDG injection, a method for measuring blood flow and metabolism in tumors could provide an important addition to the functional imaging of tumors with ^{18}F-FDG PET. A full, 1-h, dynamic ^{18}F-FDG PET acquisition is expensive making it impractical for routine practice. Accordingly, Mullani et al. developed a 2-min dynamic first-pass PET acquisition, based on a 1-compartment flow model to assess tumor blood flow BF [11].

In order to achieve K values, a dynamic PET application and computer software program are needed. However, in a study on lung cancer, it was shown that there was a strong association (r=0.83, p=0001) between K1 values obtained from dynamic FDG PET and early-phase imaging (0-2 minutes) SUV without the need for software [25]. A dynamic PET study in patients with soft tissue sarcoma also found a strong relationship between SUV obtained between 1.5-2.5 minutes and K1 values (r=0.79, p<0.05) [22]. In a study performed in patients with NSCLC, there was a strong correlation between ^{15}O water PET BF and FDG PET early-phase imaging (0-5 min) standardized uptake normalized to body surface area (SUVbsa), yet no correlation was found in 4-5–min SUV [15]. We obtained SUV_E values that reflected perfusion and were highly correlated with K1, without the use of a kinetic PET program and without the need for software, and we investigated its prognostic value by calculating its proportion with conventional imaging SUV.

We also think that the combined visual evaluation of early-phase and conventional images may contribute to the evaluation of treatment response. Perfusion-metabolism imaging allows us to see the mismatched/hypoxic areas in the tumor. In some studies, perfusion and metabolism imaging was performed before and after treatment, and it was indicated that metabolism and perfusion did not show a balanced decline due to treatment. Miles et al. followed up the chemotherapy response with conventional CT, perfusion CT, and ^{18}F FDG PET in a patient with colon cancer and liver metastasis. After the treatment, the least change was observed in metabolism (metabolism 11%, perfusion 47%, area 43%), and they suggested that the tumor might have developed an adaptation to hypoxia during the treatment process. They stated that metabolism-perfusion combined imaging would contribute to determining adaptive treatment options [26]. Again, Miles et al. evaluated the tumor response with metabolic and perfusion imaging, and concluded that the best outcome was in the group that had the balanced response in perfusion and metabolism. They proposed adaptive treatment against neovascularization in the group with reduced metabolism and unchanged or increased perfusion, and adaptive treatment against hypoxia in the group with unchanged or increased metabolism and reduced perfusion. They emphasized that the ultimate goal in the management of patients with cancer was to adapt individual patient treatment to the vascular and metabolic response exhibited by their tumors [27]. A study of rectal cancer by Willett et al. using perfusion CT and FDG-PET reported significant falls in perfusion, but no change in glucose metabolism when the VEGF antibody, bevacizumab, was given alone. A reduction in glucose metabolism was only seen when bevacizumab was given in combination with radiotherapy [28]. A study that was conducted in patients with breast cancer revealed that although chemotherapy-related metabolism decreased, perfusion might not decrease and might even increase [29]. Herbst et al. evaluated high-dose endostatin (an anti-vascular agent) response in 25 patients and reported that perfusion calculated by [^{15}O] H_2O PET decreased, yet glucose metabolism in ^{18}F FDG PET increased [30].

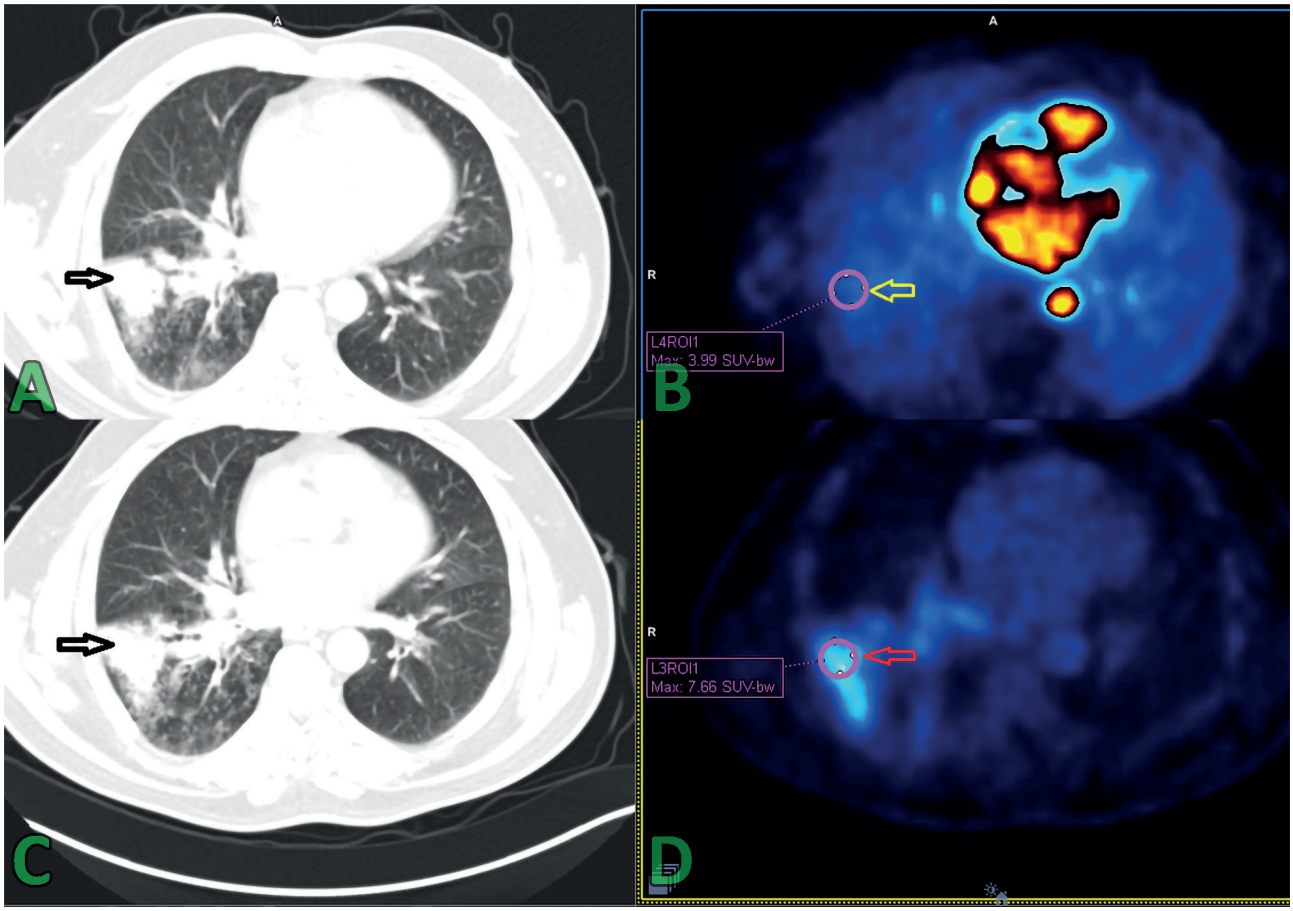

Figure 4. A 52-year-old-male with adenocarcinoma. CT (A) and PET (B) images of the early phase reveal the SUV_{max} as 3.99 (yellow arrow). On conventional imaging CT (C) and PET (D) of conventional imaging, SUV_{max} is 7.66 (red arrow). If there is early-phase imaging and conventional imaging of the patient after treatment, change in perfusion and metabolism due to treatment can be calculated and perhaps can contribute to the formation of ideas about additional treatment options.

Although not investigated in this study, we suggest that combined early-phase and conventional imaging as a developable idea can be used to evaluate metabolism and perfusion response in the follow-up of cancer treatment, similar to the above-mentioned studies. Thus, the change in early phase imaging SUV and conventional imaging SUV values calculated in pre-treatment PET can be measured after treatment (%change) and may contribute to adaptive treatment planning according to metabolism predominant, perfusion predominant or balanced responses, as described in some of the above examples (Figure 4).

We found no statistically significant correlation between early-phase imaging and conventional imaging SUV values. Tateishi et al. studied the relationship between peak attenuation (Apa) and relative flow (RF) with SUV in patients with NSCLC (tumor size: 2.6±0.2; range, 0.9-3.4 cm) and showed that both perfusion parameters of CT had a correlation with SUV [31] . Miles et al. compared standardized perfusion value (SPV) with SUV in 18 patients with NSCLC and reported that no correlation existed in the entire group of patients (n=18), albeit there was a statistically significant relation only in the group of patients whose tumor size was less than 4.5 cm^2 (n=6, mean size 2.4 cm) [32]. The authors discussed that there was a relationship between tumor perfusion and tumor metabolism and tumor size; the biologic aspect of tumor differentiated as the tumor grew, and a metabolic-perfusion difference was more prominent in large and high-grade tumors. Likewise, we divided the patients into two groups according to tumor size, and we accepted 3 cm [≤ 3 cm (n=21), and >3 cm (n=56)] as a threshold. Based on the knowledge that early-phase images reflect perfusion, our result is consistent with the above-mentioned two studies.

We found that the conventional imaging/early-phase imaging FDG uptake ratio (SUV_R) increased as tumor size increased. Our findings are consistent

with the literature showing that the metabolism-perfusion difference increases as the tumor size increases [33-35].

Our study has limitations; first of all our study is a single-center study. The reason for male dominance in the patient group can be explained by the fact that the female population smoked less in this region, and that they had a relatively low incidence of lung cancer. The main limitation of the study was the lack of data about the treatment details which could be among the reasons for the results. In addition, a lack of comparison between the baseline characteristics of the patient groups with different SUV values was absent other than tumor size.

In conclusion, the ratio of conventional imaging SUV to early phase imaging SUV was found an indicator for prognosis. Evaluating the early phase imaging, without a need for kinetic program or software, without disrupting the routine functioning of the clinic, with conventional imaging may contribute to cancer patient management. There is a need for studies with larger groups of patients.

CONFLICT of INTEREST

The authors declare that there is no conflict of interest.

REFERENCES

[1] Takeda A, Yokosuka N, Ohashi T et al. The maximum standardized uptake value (SUVmax) on FDG-PET is a strong predictor of local recurrence for localized non-small-cell lung cancer after stereotactic body radiotherapy (SBRT). Radiother Oncol. 2011; 101: 291-7.

[2] Imamura Y, Azuma K, Kurata S et al. Prognostic value of SUVmax measurements obtained by FDG-PET in patients with non-small cell lung cancer receiving chemotherapy. Lung Cancer. 2011; 71: 49-54.

[3] Kohutek ZA, Wu AJ, Zhang Z et al. FDG-PET maximum standardized uptake value is prognostic for recurrence and survival after stereotactic body radiotherapy for non-small cell lung cancer. Lung Cancer. 2015; 89: 115-20.

[4] Semenza GL. HIF-1 and tumor progression: pathophysiology and therapeutics. Trends Mol Med. 2002; 8: S62-S7.

[5] Clavo AC, Brown RS, Wahl RL. Fluorodeoxyglucose uptake in human cancer cell lines is increased by hypoxia. J Nucl Med. 1995; 36: 1625-32.

[6] Airley RE, Mobasheri A. Hypoxic regulation of glucose transport, anaerobic metabolism and angiogenesis in cancer: novel pathways and targets for anticancer therapeutics. Chemotherapy. 2007; 53: 233-56.

[7] Brown JM, Wilson WR. Exploiting tumour hypoxia in cancer treatment. Nat Rev Cancer. 2004; 4: 437-47.

[8] Held KD. Radiobiology for the Radiologist, by Eric J. Hall and Amato J. Giaccia. Radiat Res. 2006; 166: 816-7.

[9] Servagi-Vernat S, Differding S, Sterpin E et al. Hypoxia-guided adaptive radiation dose escalation in head and neck carcinoma: a planning study. Acta Oncol. 2015; 54: 1008-16.

[10] Mullani N. et al. 9: 30—9: 45: First Pass FDG Measured Blood Flow in Tumors: A Comparison with O-15 Labeled Water Measured Blood Flow. Clinical Positron Imaging. 2000; 3: 153.

[11] Mullani NA, Herbst RS, O'Neil RG, et al. Tumor blood flow measured by PET dynamic imaging of first-pass 18F-FDG uptake: a comparison with 15O-labeled water-measured blood flow. J Nucl Med. 2008; 49: 517-23.

[12] Goethals I, Hanssens S, Kortbeek K, et al. Hypothesis using dynamic 18 F-FDG PET in oncology. Eur J Nucl Med Mol Imaging. 2010; 37: 833-833.

[13] Mertens J, Ham H, De AZ, et al. Tumor perfusion using first-pass F-18 FDG PET images. Clin Nucl Med. 2012; 37: 166-7.

[14] Komar G, Kauhanen S, Liukko K et al. Decreased blood flow with increased metabolic activity: a novel sign of pancreatic tumor aggressiveness. Clin Cancer Res. 2009; 15 : 5511-7.

[15] Hoekstra CJ, Stroobants SG, Hoekstra OS, et al. Measurement of perfusion in stage IIIA-N2 non-small cell lung cancer using H215O and positron emission tomography. Clin Cancer Res. 2002; 8 : 2109-15.

[16] van Elmpt W, Zegers CM, Reymen B, et al. Multiparametric imaging of patient and tumour heterogeneity in non-small-cell lung cancer: quantification of tumour hypoxia, metabolism and perfusion. Eur J Nucl Med Mol Imaging. 2016; 43: 240-8.

[17] Carlson DJ, Yenice KM, Orton CG. Tumor hypoxia is an important mechanism of radioresistance in hypofractionated radiotherapy and must be considered in the treatment planning process. Med Phys. 2011; 38: 6347-50.

[18] Hermans R, Meijerink M, Van den Bogaert W, et al. Tumor perfusion rate determined noninvasively by dynamic computed tomography predicts outcome in head-and-neck cancer after radiotherapy. Int. J. Radiat. Oncol. Biol. Phys. 2003; 57: 1351-6.

[19] Park M-S, Klotz E, Kim M-J et al. Perfusion CT: noninvasive surrogate marker for stratification of pancreatic cancer response to concurrent chemo-and radiation therapy. Radiology. 2009; 250: 110-7.

[20] Aoki M, Akimoto H, Sato M, et al. Impact of pretreatment whole-tumor perfusion computed tomography and 18F-fluorodeoxyglucose positron emission tomography/ computed tomography measurements on local control of non–small cell lung cancer treated with stereotactic body radiotherapy. J Radiat Res. 2016; 57: 533-40.

[21] Mankoff DA, Dunnwald LK, Gralow JR, et al. Blood flow and metabolism in locally advanced breast cancer: relationship to response to therapy. J Nucl Med. 2002; 43: 500-9.

[22] Rusten E, Rødal J, Revheim ME, et al. Quantitative dynamic 18FDG-PET and tracer kinetic analysis of soft tissue sarcomas. Acta Oncol. 2013; 52: 1160-7.

[23] Okazumi S, Dimitrakopoulou-Strauss A, Schwarzbach M, et al. Quantitative, dynamic 18F-FDG-PET for the evaluation of soft tissue sarcomas: relation to differential diagnosis, tumor grading and prediction of prognosis. Hell J Nucl Med. 2009; 12: 223-8.

[24] Strauss LG, Koczan D, Klippel S, et al. Impact of angiogenesis-related gene expression on the tracer kinetics of 18F-FDG in colorectal tumors. J Nucl Med. 2008; 49: 1238-44.

[25] TUNCEL, M., et al. Practical measures of dynamic 18 FDG time-activiy curves. Eur J Nucl Med Mol Imaging. 2015 (suppl 1): p. S375-S375.

[26] Miles K, Williams R. Warburg revisited: imaging tumour blood flow and metabolism. Cancer Imaging. 2008; 8: 81.

[27] Miles K, Charnsangavej C, Cuenod C. CT perfusion of lympth nodes. Multi-Detector Computed Tomography in Oncology. CRC Press; 2007. p. 179-88.

[28] Willett CG, Boucher Y, Di Tomaso E et al. Direct evidence that the VEGF-specific antibody bevacizumab has antivascular effects in human rectal cancer. Nat Med. 2004; 10 : 145-7.

[29] Mankoff DA, Dunnwald LK, Gralow JR et al. Changes in blood flow and metabolism in locally advanced breast cancer treated with neoadjuvant chemotherapy. J Nucl Med. 2003; 44: 1806-14.

[30] Herbst RS, Mullani NA, Davis DW et al. Development of biologic markers of response and assessment of antiangiogenic activity in a clinical trial of human recombinant endostatin. J Clin Oncol. 2002; 20: 3804-14.

[31] Tateishi U, Nishihara H, Tsukamoto E et al. Lung tumors evaluated with FDG-PET and dynamic CT: the relationship between vascular density and glucose metabolism. J Comput Assist Tomogr. 2002; 26: 185-90.

[32] Miles KA, Griffiths MR, Keith CJ. Blood flow-metabolic relationships are dependent on tumour size in non-small cell lung cancer: a study using quantitative contrast-enhanced computer tomography and positron emission tomography. Eur J Nucl Med Mol Imaging. 2006; 33: 22-8.

[33] Kiessling F, Boese J, Corvinus C et al. Perfusion CT in patients with advanced bronchial carcinomas: a novel chance for characterization and treatment monitoring? Eur Radiol. 2004; 14: 1226-33.

[34] Fukuda K, Taniguchi H, Koh T et al. Relationships between oxygen and glucose metabolism in human liver tumours: positron emission tomography using (15)O and (18) F-deoxyglucose. Nucl Med Commun. 2004; 25: 577-83.

[35] Stewart EE, Chen X, Hadway J et al. Correlation between hepatic tumor blood flow and glucose utilization in a rabbit liver tumor model. Radiology. 2006; 239: 740-50.